Scientific paper

Adsorptive Removal of Fluoride from Aqueous Solution by Biogenic Iron Permeated Activated Carbon Derived from Sweet Lime Waste

Mohd. Ibrahim,[1] Adil Siddique,[1] Lata Verma,[1] Jiwan Singh[1,*] and Janardhan Reddy Koduru[2,*]

[1] *Department of Environmental Science, Babasaheb Bhimrao Ambedkar University, Lucknow-226025, India*

[2] *Department of Environmental Engineering, Kwangwoon University, Seoul 139-701, Republic of Korea*

* *Corresponding author: E-mail: jiwansingh95@gmail.com reddyjchem@gmail.com*

Received: 09-14-2018

Abstract

In this study, biogenic activated carbon were successfully synthesized from *Citrus limetta* pulp residue, and applied to remove fluoride from an aqueous solution. For the synthesis activated carbon of biosorbents, raw materials were heated in muffle furnace at two different temperatures i.e. (250 °C and 500 °C) and were noted as ACP-250 and ACP-500. The prepared biosorbents were characterized through scanning electron microscopy (SEM), Fourier transform infrared (FTIR), and X-ray diffraction (XRD). Batch adsorption studies were performed with varying temperature, dosage, pH, and various initial concentrations. Adsorption isotherms and the reaction kinetics were also analyzed in order to understand the adsorption mechanism. The results of this study shows that the maximum removal achieved was approximately (86 and 82) % of ACP-500 and ACP-250, respectively. The isotherm results show that the Langmuir isotherm model fitted better, with monolayer adsorption capacity of 12.6 mg/g of fluoride. However, for kinetic study, the pseudo-second-order kinetics fitted well. The synthesized materials at different temperature were highly effective for the removal of fluoride from water, with reusability of three to four times.

Keywords: Sweet lime waste; adsorption; fluoride; isotherm; thermodynamic; cost analysis.

1. Introduction

The presence of fluoride in drinking water offerings a severe complication worldwide[1]. In India, more than 95% of rural and (30–40) % of the urban population are dependent on groundwater.[2] The higher amount of fluoride in groundwater is dangerous for drinking purposes. Normally, fluoride is released in groundwater through the slow leaching of fluorine-containing rock,[3] and of several minerals viz., topaz, biotite, fluorite, and their corresponding host rock, such as basalt, syenite, granite, etc.[4] Moreover, while the natural geological source contributes fluoride to groundwater, several industries also contribute to fluoride contamination.[5] According to Shen et al.[6] some industries generate fluoride in the environment, and discharge higher fluoride concentration than natural geological dissolution, ranging (10–1,000) mg/L.[7] More than 200 million people worldwide are affected by higher fluoride concentration that exceeds the WHO guideline of 1.5 mg/L.[8] Contamination of fluoride occurs in different parts of India, including Andhra Pradesh, Assam, Gujarat, Haryana, Rajasthan, and Uttar Pradesh.[9] The amount of fluoride in groundwater in some parts of India is above 30 mg/L.[10] The impact of fluoride in drinking water depends on the concentration and duration of continuous uptake, and can be useful or harmful to humankind. Even a small concentration of fluoride in water has a significant effect on dental caries, mainly among children.[11] An excessive amount of fluoride causes various diseases, such as osteoporosis, arthritis, brittle bones, cancer, infertility, brain damage, Alzheimer syndrome, and thyroid disorder.[12] Among these diseases, fluorosis is one of the most common diseases in human who are consuming fluoride regularly, also causing mottling of the teeth, and embrittlement of the bones of human.[13] Hence, there is necessity to treat of water contaminated with fluoride before drink or release to environment.

Many technologies, such as chemical precipitation, coagulation, ion exchange, electrocoagulation, nanofiltration, catalytic ozonation, and electrochemical oxidation[14–18] and Donnan dialysis[19] have been used for the fluoridation of water. However those methods have limitations in terms of high operational and maintenance cost, and generation of waste. The adsorptive removal of fluoride has been considered one of the most facile, cost-effective, and eco-friendly techniques among the various defluoridation technologies.[14–20] Several adsorbents, including various conventional and non-convention sorbents/biosorbents, such as red mud, bone char, rare earth oxides, zeolite, citrus lemon leaves, rice husk ash, peepal leaf, musambi peel, banana peel, and laterite soils, have been reported for the defluoridation of water.[21] However, most biosorbents have low fluoride removal abilities to treat fluoride-contaminated groundwater. Therefore, the development of better bioadsorbents with superior adsorption capacities for fluoride is still needed. Given the higher cost of production, presented agriculture solid waste is being intensively studied for the production of low-cost activated carbons. Waste materials that are converted into activated carbon improve economic value, reduce the cost of waste disposal, and potentially offer a cheap alternative to the current viable sample.[22]

However, functionalizing iron-oxide nanoparticles with parent biosorbent, improving adsorption capacity, selectivity and stability levels of tested materials.[23] So, these functionalized activated carbons with iron oxide are great interest for removing pollutants from water. Moreover, the modification of biogenic activated carbon with iron oxide that can enhances its adsorption ability and selectivity of parent material.[24]

In the present study, *Citrus limetta* pulp was used for the synthesis of biogenic activated carbon permeated with iron. It is valuable waste material that is thrown away from the juice industry, and engenders land space occupation and pollution with phenolic compounds, due to the dumping of wastes. Natural biomaterial waste *citrus limetta* pulp was used as a template, and $FeCl_3.6H_2O$ was used for the iron precursor source to develop magnetic properties in both the adsorbents for the removal of fluoride from an aqueous solution. Two adsorbents were prepared at two different temperatures of (250 and 500) °C for the potential application for fluoride removal.

2. Materials and Methods

2. 1. Chemicals

For the purpose of the research work, analytical grade chemicals were used. These chemicals were anhydrous sodium fluoride (NaF), iron chloride hexahydrate ($FeCl_3.\ 6H_2O$), sodium hydroxide (NaOH), hydrochloric acid (HCl), and Ionic Strength Adjustment (ISA) Solution, purchased from Fisher Scientific (a part of Thermos Fisher Scientific).

2. 2. Preparation of Pulp powder

Citrus limetta (sweet lime) pulp waste was collected from a local juice seller nearby the area of BBAU, Lucknow, India. Plenty of water was required for the washing of raw material so firstly the tap water was used for washing of collected pulp material to eliminate the dust particles and other adherence from the surface of collected material, af-

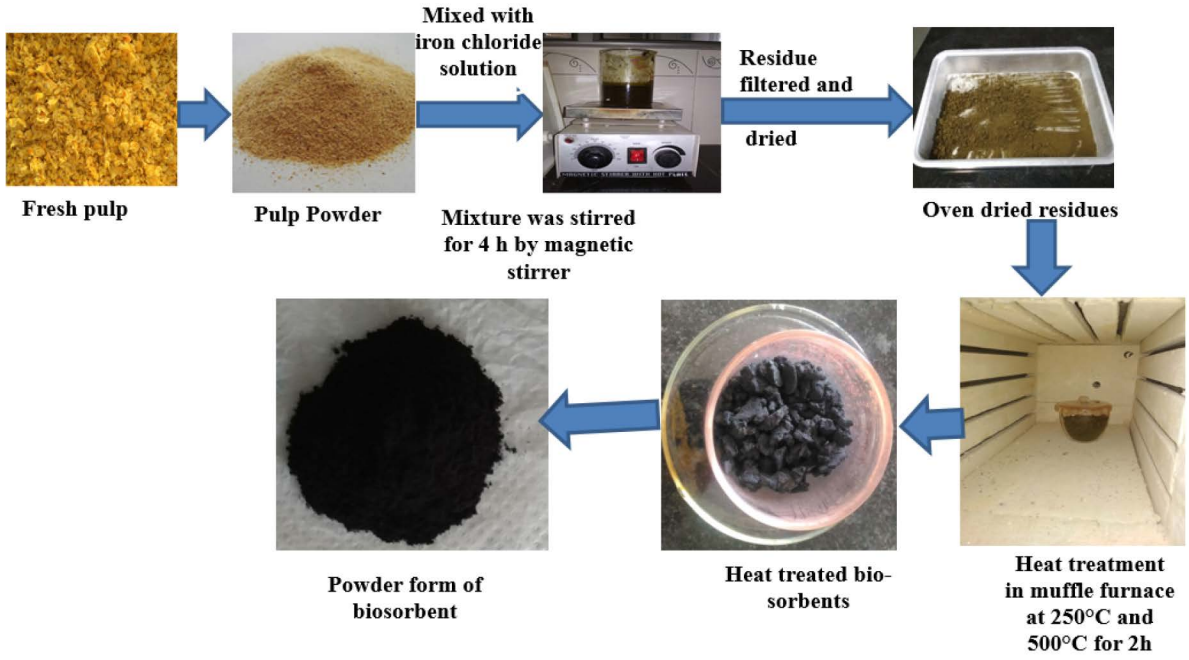

Figure 1. A flowchart for the synthesis of biogenic iron permeated activated carbon (ACP- 250 and ACP-500).

ter that the material was washed with distilled water atleast three times. The study area is not affected by fluoride. Pulp waste was chopped in small pieces, and then air-dried. The dried pulp was crushed and ground with the help of grinder, and finally, powder forms were obtained by sieving with 250 μm sieve. The sieved powder was used for the preparation of activated carbon (bio-sorbents).

2. 3. Synthesis of Biogenic Iron Permeated Activated Carbon

Bioadsorbents were prepared according to the method given by Lunge.[25] The details of synthesis are that 15 g of Iron chloride hexahydrate ($FeCl_3.6H_2O$) was dissolved in 150 mL of distilled water, and 30 g of fine pulp powder was added and stirred for 4 h, and kept overnight, then, the solid materials were separated by vacuum pump filtration, followed by oven drying at 105 °C for 4 h. The iron-treated material was heated in a muffle furnace (Model No.11C 106B; ICOAN Instruments Company, India) at two different temperatures *i.e.* (250 and 500) °C for 2 h.

Iron chloride hexahydrate was used for the preparation of ACP to develop magnetic properties and acidic nature to the ACP. Moreover, the addition of $FeCl_3$ can be improve positive surface which is favorable for adsorption negative charge fluoride. The heated material was washed with double distilled water, and then dried. A black color final product was obtained named as activated carbon of pulp, denoted as ACP-250 and ACP-500. These materials were ground and made uniform using mortar and pestle, and applied for the fluoride removal. Fig. 1 shows the different steps in the synthesis of bioadsorbents.

2. 4. Preparation of Standard Solution of Fluoride and its Determination

For the purpose of batch experiment, different concentrations of fluoride solution were prepared by diluting the stock solution of 1,000 mg/L concentration of F^- (a stock solution prepared by NaF salt). The concentration of fluoride and pH of the solution was determined by digital Ion-pH meter (EUTECH Handheld Meter Kit; Thermo Scientific).

2. 5. Spectroscopy and Microscopy Identification of Adsorbents

The XRD configuration of the biosorbent was attained by X-ray Diffractometer (PW 30 40/60, PANalytical, Netherlands), which was used to analyze the phase and structure of both biosorbents. Surface morphology, structure, and elemental composition of the biosorbents were obtained with SEM equipped with EDX (JSM 6490-LV, JEOL, Japan). Various functional groups analysis of the adsorbents were analyzed by using FTIR Spectrophotometry (NICOLETTM 6700, Thermo Scientific, USA) with KBr at a ratio of 1:200, and the mixture was pressed, as reference material and spectra were detailed in the region of (400 to 4,000) cm^{-1}. The synthesized bioadsorbents were analyzed for surface charge i.e. zero point charge (pHzpc), by the method reported by Sharma.[10]

2. 6. Procedure for Adsorptive Removal of Fluoride

A 50 mL of fluoride solution (10 mg/L) was mixed with 1 g/L dose of **biogenic activated carbon** material, and kept in horizontal water bath shaker (LI-WBIS-20; Labard Instruchem. Pvt. Ltd) at 25 °C for 5 h for shaking at 100 rpm. Samples were collected at different time intervals. The optimum conditions for maximum removal of fluoride using biadsorbents have been estimated by observing the effect of contact time of (30–300) min, initial pH of (4–10), adsorbent dose of (0.5–3.0) g/L, temperature of (25–55 °C), and initial fluoride concentrations of (5–30) mg/L at 100 rpm; then the flasks were taken at different time intervals from the water bath shaker, followed by filtration through Whatman 42 filter paper. The filtrate was used for the determination of the remaining fluoride ions using ion selective electrode contain digital Ion-pH meter. The batch study was carried out in duplicate, and average values were calculated, and taken as the final value.

The fluoride removal efficiency using biosorbents (ACP-250 and ACP-500) during adsorption was calculated as follows:

$$\text{Removal efficiency } (\%) = ((C_0 - C_i)/C_0) \times 100 \quad (1)$$

The amount of adsorbed F^- per unit mass of adsorbent was obtained using the formula:

$$q_e = (C_0 - C_e)V/W \quad (2)$$

Where, q_e is the adsorption capacity of F^- (mg/g); C_o is the initial F^- concentration (mg/L); C_e is the F^- concentration at equilibrium (mg/L); W is the adsorbent mass (g), and V is the volume of F^- solution (L).

3. Results and Discussion

3. 1. Characterization of Biosorbent

3. 1. 1. Zero Point Charge (pH_{zpc})

The pH_{zpc} of an adsorbing material is a significant parameter that regulates the pH at which the adsorbent surface has net electrical charge neutral. In the case pH of solution < pHzpc, the adsorbent surface charge is positive to attract negative ions; however, when pH of solution > pHzpc, then the surface charge of adsorbent is negative to attract positive ions.[26] The pHzpc of the prepared materials, ACP-250 and ACP-500 have been found to be 2.66

and 3.06, respectively. From the results, both biosorbents may have more acidic functional groups such as carboxylic, phenolic groups etc., on their surfaces. It is fact that the biosorbents show different pHzpc values may be due to the presence or absences of acidic groups. These groups decrease with increasing carbonization temperature. However, during the burning of adsorbent, acidic metal oxides formed on the adsorbent surface. The pHzpc value of an aqueous solution plays an important role in the surface charge of the biosorbent.

3. 1. 2. SEM Analysis

Fig. 2 (a)–(d) show the SEM images of ACP-250 and ACP-500, and reveal a rough surface with porous and crystalline structure for both biosorbents, which may be favorable for fluoride adsorption. The morphology of the two biosorbents was different, because of the thermal treatment at different temperatures. Furthermore, the adsorption of fluoride ion onto ACP-250 and ACP-500 was established by EDX analysis. Fig. 2 (e) and (f) show the EDX spectra of ACP-250 and ACP-500, which indicate

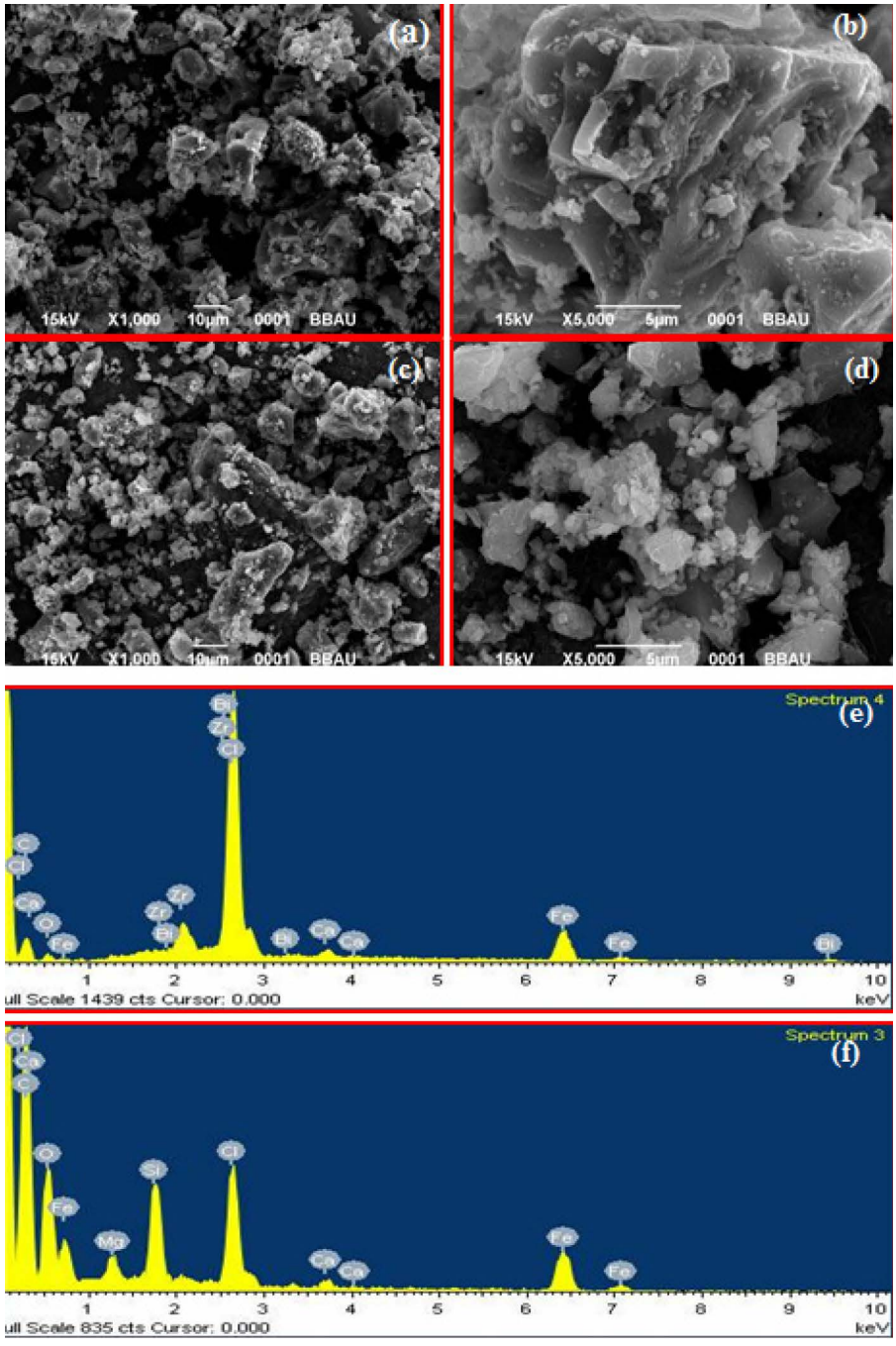

Figure 2. SEM images of (a) and (b) ACP-250, (c) and (d) ACP-500; and EDX spectra of (e) ACP-250, and (f) ACP-500.

the higher percentage of carbon in ACP- 500 (57.98%), as compared to ACP-250 (50.27%). Iron was present in both materials, and Table S1 shows the weight percentage of ACP.

3. 1. 3. FTIR analysis of biosorbent

The FT-IR spectra of ACP-250 and ACP-500 display numerous characteristic peaks. Figures 3 (a) and (b) show the FTIR spectra of ACP before and after fluoride adsorption, which display a number of adsorption peaks in the range (4,000–500) cm^{-1}, which confirm the presence of different functional groups on the surface of biosorbents. The broad band peaks at (3,320.0–3,340.0) cm^{-1} were attributed to stretching vibrations in the hydroxyl group.[27] The peaks that occur in the range (2,852.0–3,000.0) cm^{-1} were attributed to –C–H stretching in the hetero aromatic ring, with both alkyl and ethylene group in the side chain. Symmetric C–H stretching vibration of aliphatic acid is indicated by peaks at 2,921.9 cm^{-1}.[28] The peaks located in the range (1,690.0–1,710.0) cm^{-1} relate to the asymmetric stretching vibration of the ionic carboxylic group ($–COO^-$).[27] Wavenumber ranges from 1033–1500 cm^{-1} represents C-N streching in aromatic amines, CH_2-O-O stretching in primary alcohol, OH group of carboxylic acids and CF_3 group attached to benzene ring.[29] The sharp peak at (500–800) cm^{-1} was related to the C–O [30] and metal–oxygen (Fe–O) bonds [31]. The presence of Fe–O band spectra before and after adsorption shows the Fe_3O_4 group. Fig.3(b) shows the FTIR spectra of ACP-500 and it was observed that the change in the intensity of the peaks confirms the adsorption of fluoride.

3. 1. 4. XRD Analysis

Figure 3 c shows the X-Diffraction patterns of ACP-250 and ACP-500. Different diffraction peaks are observed on ACP-500, which indicate its crystalline structure; however, in the case of ACP-250, the absence of diffraction peaks is observed, which indicates its amorphous structure.

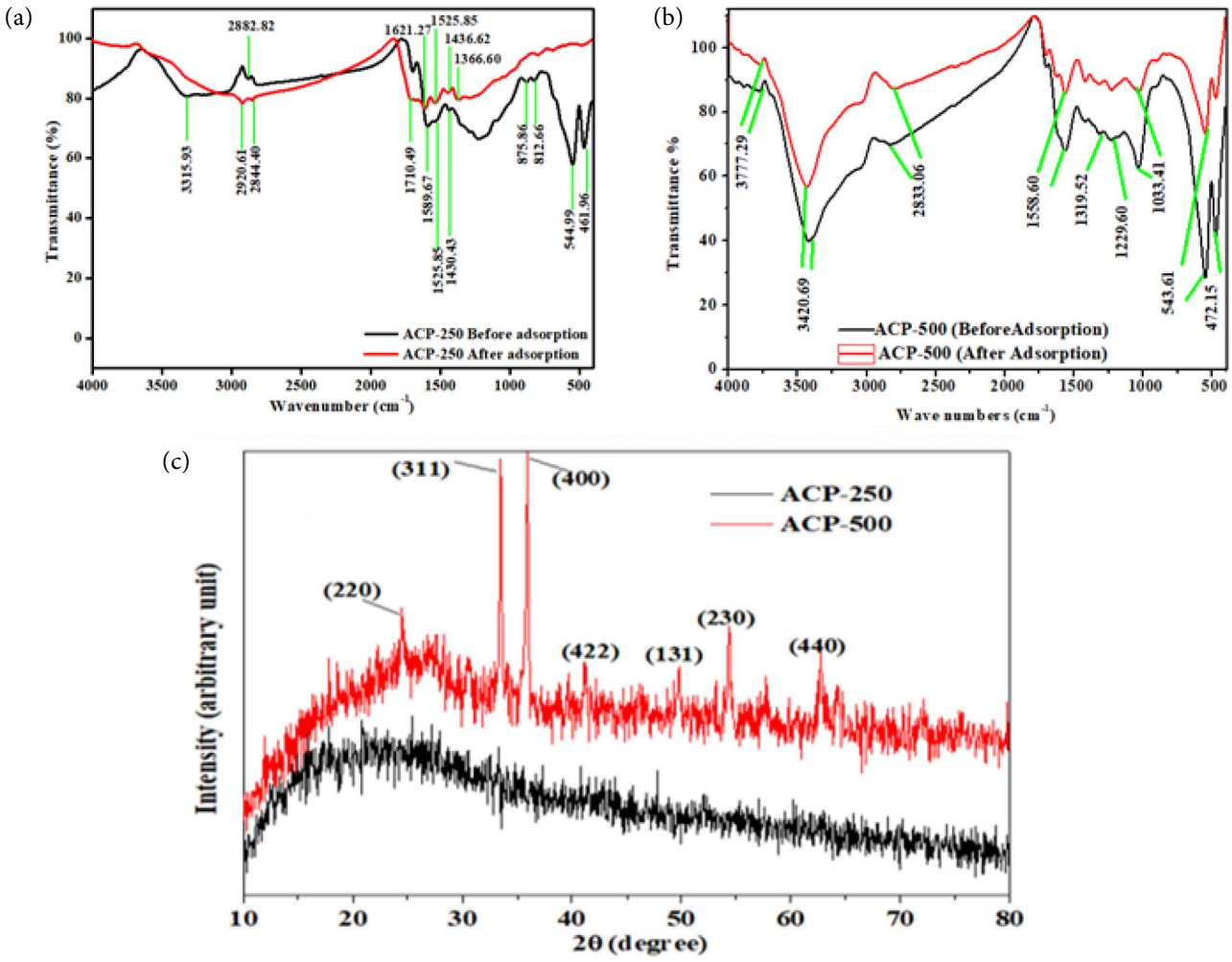

Figure 3. FTIR spectra of (a) and (b) before adsorption and after adsorption of ACP-250 and ACP-500, and (c) XRD spectra of ACP-250 and ACP-500.

Consequently, the removal of fluoride from water by applying ACP-500 was found to be higher than that by ACP-250. The XRD pattern of ACP-500 reveals peaks at 2θ = (24.55, 33.52, 36.04, 41.23, and 62.77°) that were assignable by their indices (220), (311), (400), (422), and (440), respectively. [32–33] All these peaks are in accord with the database in JCPDS file (82-1533), and represent the iron oxides (for example Fe_3O_4). The diffraction peaks at (49.88 and 54.29) corresponding to the (131) and (230) planes, respectively, represent Fe_3C. Carbides of iron may be classified into two categories on the basis of the location of carbon atoms present either in trigonal-prismatic interstices (Fe_3C and Fe_5C_2), or octahedral interstices (e.g., Fe_2C, $Fe_{2.2}C$). The formation of the carbides may increase the mechanical strength of the synthesized nano/micro size material.[34]

3. 2. Fluoride Adsorption Study

3. 2. 1. Effect of Contact Time

Figures S1 (a)–(d) show the removal percentage of ACP-250 and ACP-500 toward fluoride ion with time. It was observed that in the first 30 minute of contact time, about (35 and 58.5)% fluoride adsorption was observed by ACP-250 and ACP-500, respectively; and afterward, the adsorption rate slowed down with contact time. During the early stage of the adsorption experiment, many vacant sites are available on the surface of the adsorbent for the removal of fluoride. After a certain period of time, fluoride ion is difficult to attach to the surface of the adsorbent, because of the repulsive force between the adsorbed fluoride ion on the surface, and fluoride ion in the aqueous solution. The removal of fluoride increased along with time, and then progressively reached equilibrium at 180 min. Therefore, 180 min is considered the minimum contact time to maximum removal of fluoride from the water. A similar result was also reported by Dwivedi [35] and Singh and Majumder.[36]

3. 2. 2. Effect of the Amount of Biosorbents

The removal of fluoride ions by ACP-250 and ACP-500 was performed at different adsorbent doses i.e. (0.5, 1.0, 2.0, and 3.0) g/L, while keeping all other parameters constant, such as pH (6.6±0.5), initial fluoride concentration 10 mg/L, temperature 25 °C, with different time intervals i.e. 30, 60, 120, 180, 240, and 300 min. Figures S1 (c) and (d) indicates the removal percentage of fluoride of both of the adsorbents. The adsorption of fluoride by adsorbent was observed to be increases from 32.5 to 47% for 0.5 g/L, and the maximum removal was observed 70% in case of 1.0 g/L. While in the case of 2.0 and 3.0 g/L, the adsorption removal gradually decrease from 41 to 29.5% and 49.2 to 39%, respectively for both the bioadsorbents. The highest removal percentage was shown for both bioadsorbents at 1.0 g/L dosage. The increase of the percentage of fluoride removal with increasing biosorbent dose might be due to the availability of more active site on the adsorbents surface for the binding of fluoride ions with the increased surface area,[37] While further increase of the biosorbent dose, the removal percentage was not increased, because of the partial aggregation of biomass, which resulted in decrease in the active surface area of both biosorbents for the adsorption.[38]

3. 2. 3. The Effect of pH Values

The pH of a solution is a critical aspect that affects the adsorption process, due to its close relationship with the surface charge of the biosorbents, and the ionization potential of fluoride ion; therefore fluoride adsorption on adsorbent was performed at different pH values ranging (4–10), while keeping all other parameters constant. The required pH was adjusted by adding 0.1 N NaOH or 0.1 N HCl. Fig. S1 (b) shows the effect of pH on the removal of fluoride. The result shows that the adsorption of fluoride on ACP-250 and ACP-500 observed a maximum of 76.5 and 74% respectively, at pH 4. It was perceived that the removal of fluoride is extremely sensitive to the change in pH of the solution. It was also observed that fluoride adsorption decreased approximately (44 and 26.4) % for ACP-250 and ACP-500, respectively, with increasing pH of the solution from (4 to 10). Fluoride adsorption decreases may be due to the following facts: (i) the negative charge increased on the surface of adsorbent as increased pH (> pHzpc is around 3.0 for both adsorbents) of solution, which reduces adsorption of the fluoride ions due to electrostatic repulsion; and (ii) enhancement of OH– ions reduces the adsorption of fluoride ions, as it increases the competition for adsorption sites.[39]

3. 2. 4. Effect of Various Fluoride Concentrations on the Adsorption Process

The effects of various fluoride concentrations on its removal were studied at different concentrations in the range (1–30) mg/L with keeping all the other parameters constant, such as pH (6.6±1), temperature (25±1) °C, with different time intervals *i.e.* 30, 60, 120,180, 240, and 300 min, and shaking speed 100 rpm. Fig. 4 (a) and (b) show the removal percentage of fluoride. The results show that when an initial concentration of fluoride increased from (1 to 30) mg/L, the removal percentage decreased from (80 to 24) % for ACP-250, and (86 to 38.33) % for ACP-500. This might have happened because of the fixed number of active sites of the adsorbent, which might be saturated at a certain concentration.

3. 2. 5. Effect of Temperature

Temperature is an essential parameter for the adsorption mechanism. Temperature determines the type of relations between the biosorbent and fluoride ions. If the removal percentage decreases with enhancing the tempera-

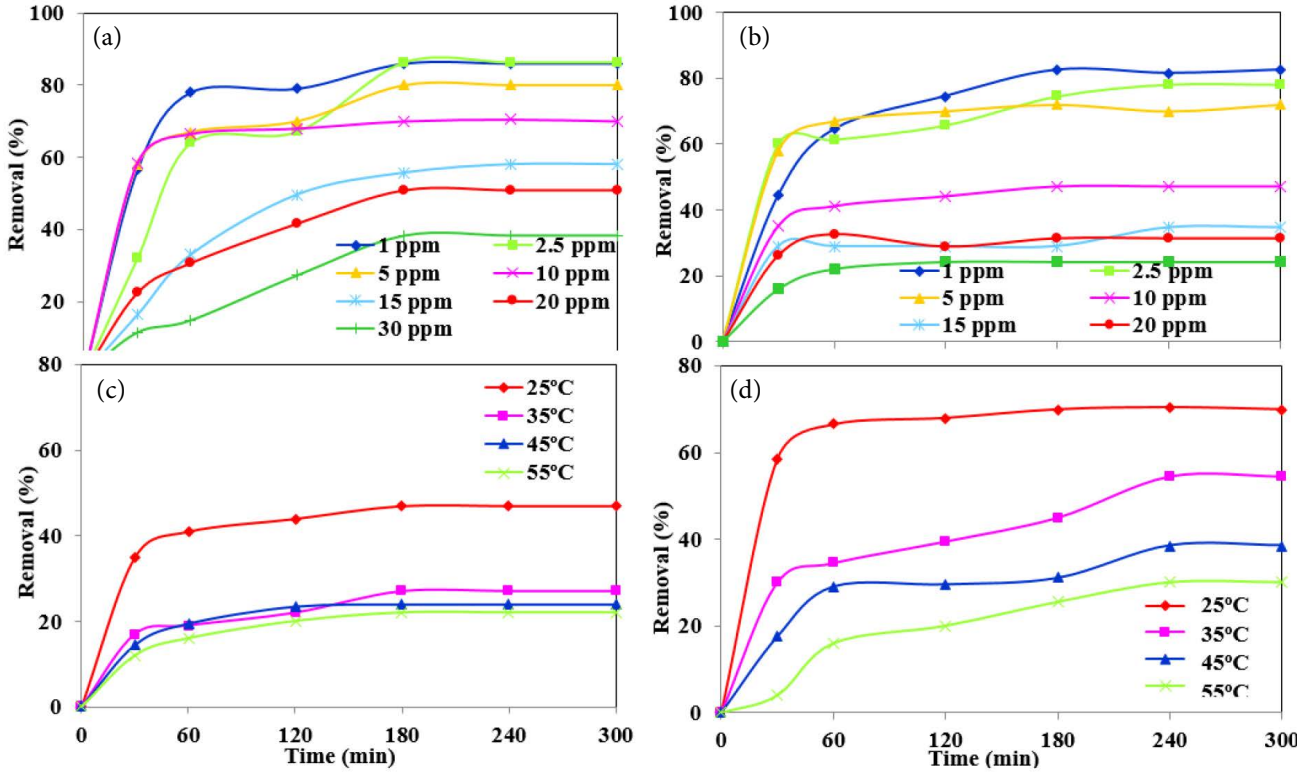

Figure 4. Effect of various parameters (a) and (b) initial fluoride concentration, (c) and (d) temperature of ACP-250 and ACP-500 for the removal of fluoride.

ture, this may represent physical adsorption or exothermic process[2]. In the present study, the impact of temperature on fluoride adsorption by ACP-250 and ACP-500 was studied at four different temperatures of (25, 35, 45, and 55) °C, while keeping all the other parameters constant. Fig. 4 (c) and (d) show the removal percentage of fluoride. The removal percentage of fluoride was observed to decrease with increase of the temperature of the solution. This represents that the fluoride removal from aqueous solution by both biosorbents is an exothermic process.[40] Further it is proved by thermodynamic studies at section 3.5.

3. 3. Adsorption Isotherm Studies

An adsorption isotherm defines the interaction between pollutant and adsorbent with adsorption properties and equilibrium information at equilibrium, a point where no further adsorption take place. To understand the nature of the interaction between the adsorbent and amount of adsorbate at a constant temperature, the adsorption isotherm is applied.[21] In the present work, to understand the adsorption behavior, the Langmuir and Freundlich isotherm model were applied.[41–42]

3. 3. 1. Langmuir Isotherm Model

The Langmuir adsorption isotherm model describes a monolayer with homogeneous adsorption, in which all sites of the adsorbent hold an equal affinity for the pollutant.[43] This model also describes an equilibrium saturation point, where no further adsorption can take place.[44–45] The monolayer adsorption model is given as Eq. (3).

$$\frac{C_e}{q_e} = \frac{1}{Q_0} + \frac{1}{bQ_0C_e} \tag{3}$$

where, q_e is the amount of F^- adsorbed per unit mass of adsorbent (mg g^{-1}); Q_0 and b are the Langmuir constant concerning the adsorption capacity (mg/g) and the binding energy constant (L/ mg), respectively. The values of Q_0 and b can be obtained using linear plot between C_e/q_e and $1/C_e$ at different fluoride concentrations (Figs. 5a and b). The Langmuir isotherm is stated as a dimensionless constant (R_L), and also denoted as a separation factor that can be calculated by applying the following equation.

$$R_L = \frac{1}{1 + bC_0} \tag{4}$$

Where, C_o is the initial fluoride concentration (mg L^{-1}), and the value of R_L indicates the adsorption process i.e. if the value of R_L lies between 0 and 1, then the adsorption process is favorable, R_L=1 signifies linear adsorption; if R_L=0, the adsorption process is irreversible; and $R_L > 1$ represents uncomplimentary adsorption, while favorable ($0 < R_L < 1$). Table 1 shows the R_L values ($0 < R_L < 1$) for both materials.

3. 3. 2. Freundlich Isotherm Model

The Freundlich adsorption isotherm describes the reversible, as well as non-ideal, adsorption. This model has been used only for multilayer adsorption with different binding energy spectra. The linear form of the Freundlich isotherm equation is given below:

$$log\ q_e = log\ K_F + \frac{1}{n}\ log\ C_e \quad (5)$$

Where, K_f and n are the Freundlich isotherm constants that represent the adsorption capacity and adsorption intensity of the fluoride ions on the biosorbents. These values can be obtained from the linear plot of ln q_e vs. ln C_e. The values of the Freundlich constants

3. 4. 1. Kinetics Studies

Adsorption kinetics studies describe the adsorption rate and mechanism of fluoride adsorption on biosorbents. Two different types of kinetics model viz, the Lagergren first-order kinetics model and the pseudo second kinetics model were applied to understand the kinetics of fluoride adsorption. The Lagergren pseudo- first-order by Ho and McKay [46] and pseudo second kinetics model [47] are expressed as Eqs. (6) and (7), respectively.

$$log\ (q_e - q_t) = log\ q_e - \frac{k_1 t}{2.303}\ l \quad (6)$$

$$\frac{t}{q_t} = \frac{1}{k_2 q_e 2} + \frac{t}{q_e} \quad (7)$$

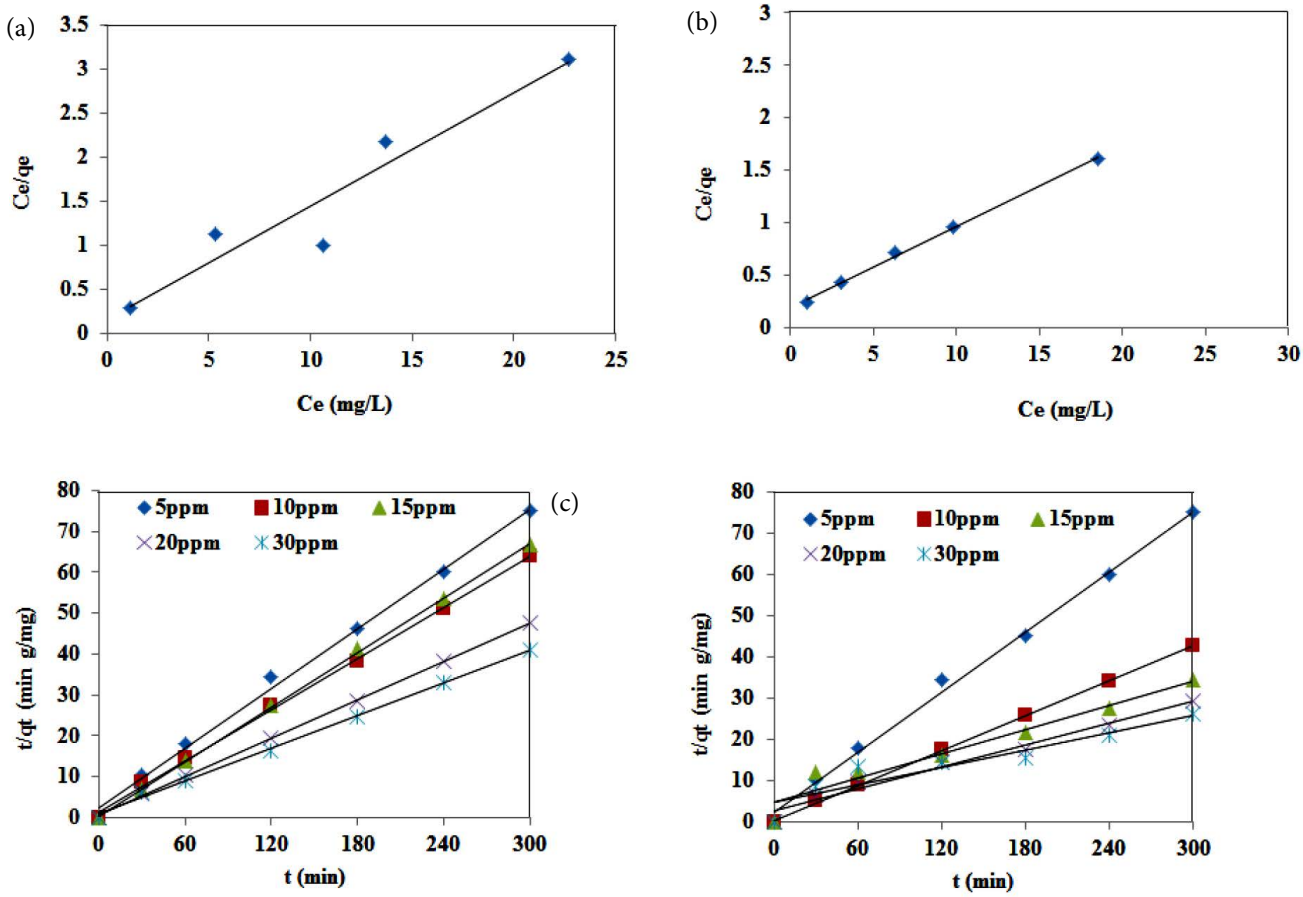

Figure 5. Adsorption isotherm and kinetics of fluoride onto ACP-250 and ACP-500 for (a) and (b) the Langmuir isotherm, and (c) and (d) second order kinetics.

K_f are (3.5886 and 4.2833) for ACP-250 and ACP-500, respectively. Table 1 shows that the values of 1/n are (5.4347 and 2.7593) for ACP- 250 and ACP-500, respectively. The results show that fluoride adsorption follows the monolayer Langmuir isotherms (R^2= 0.9772 for ACP-250, and 0.9963 for ACP-500).

where, k_1 and k_2 are the rate constants of the pseudo first order and pseudo second order kinetics, respectively; q_e (mg g^{-1}) is the adsorption capacity of the biosorbent at equilibrium, and q_t (mg g^1) is the amount of fluoride adsorbed on the adsorbent surface at time t (min^{-1}). The values of k_1, k_2, and q_e were obtained from the linear plot of log (q_e–q_t) vs. t and t/q_t vs. t.

Table 1: Isotherms Parameters for adsorption of fluoride on the ACP-250 and ACP-500

Isotherms	Parameters	Values	
Langmuir		**ACP-250**	**ACP-500**
	Q_O(mg/g)	7.5757	12.6262
	b(L/mg)	0.4404	0.4634
	R_L	0.6942	0.6833
Freundlich	R^2	0.9772	0.9963
	k_f(mg/g)	2.2344	3.2433
	N	2.4324	1.9531
	R^2	0.9353	0.9513

Table 2 lists the results of the Lagergren first-order kinetics and pseudo second kinetics model (Figures 5 (c and d)) and their regression coefficient (R^2). Pseudo-First-order theoretical adsorption capacity (mg/g) of fluoride was increased from 0.83 mg/g to 7.3 mg/g for ACP-250 and from 0.57 mg/g to 11.6 mg/g for ACP-500 with increasing concentration of fluoride from 1 mg/L to 30 mg/L. However, pseudo-second-order theoretical adsorption capacity (mg/g) of fluoride was also increased for both adsorbents ACP-250 and ACP-500, adsorption capacity for ACP-250 was almost similar to pseudo-first-order theoretical adsorption capacity. However, it was increased from 0.89 mg/g to 14.3 mg/g for ACP-500 with increasing concentration of fluoride from 1 mg/L to 30 mg/L. In comparison of the two models, the pseudo-second-order kinetics model fitted well with the adsorption data, as compared to the pseudo-first order kinetics model.

3. 4. 2 Intra-Particle Diffusion Model (IPDM)

IPDM represents the three steps for the adsorption of contaminant on to the surface of adsorbent,[48] in the

Table 2: Kinetics parameters of Pseudo first, Pseudo second and Intraparticle diffusion model for fluoride adsorption on ACP-250 and ACP-500

Pseudo First Order						
	ACP-250			**ACP-500**		
Co(mg/L)	**Qe (mg g^{-1})**	**$k_{1\ ads}$ (min^{-1})**	**R^2**	**Qe (mg g^{-1})**	**$k_{1\ ads}$ (min^{-1})**	**R^2**
1	0.825	–0.00326	0.9091	0.5757	–0.0039	0.8007
2.5	0.825	–0.00287	0.6926	1.8513	–0.0024	0.8405
5	3.6	–0.00243	0.6608	2.5153	–0.003	0.7729
10	4.7	–0.00408	0.8914	3.8010	–0.0053	0.8425
15	5.2	–0.00126	0.3642	10.0855	–0.0034	0.9923
20	6.3	–0.00343	0.7567	9.4566	–0.0026	0.9901
30	7.3	–0.0076	0.9957	11.6064	–0.0019	0.9787
Pseudo Second Order						
	ACP-250			**ACP-500**		
Co(mg/L)	**Qe (mg g^{-1})**	**$K_{2\ ads}$ (min^{-1})**	**R^2**	**Qe (mg g^{-1})**	**$K_{2\ ads}$ (min^{-1})**	**R^2**
1	0.825	0.3755	0.9452	0.8858	0.1288	0.9974
2.5	1.865	0.04817	0.9941	2.3889	0.0135	0.9699
5	3.6	0.07282	0.9992	4.1220	0.00473	0.9963
10	4.7	0.03008	0.9986	7.1022	0.04044	0.9996
15	5.2	0.01738	0.9952	10.2040	0.00204	0.9391
20	6.3	0.05227	0.9984	11.2612	0.00293	0.9765
30	7.3	0.02057	0.9978	14.3061	0.00095	0.8763
Intraparticle Diffusion						
	ACP-250			**ACP-500**		
Co(mg/L)	**Kid(mg $g^{1}min^{-1}$)**	**C(mg^{-1})**	**R^2**	**Kid(mg g^{1} min^{-1})**	**C(mg^{-1})**	**R^2**
1	0.0478	0.076	0.9302	0.0456	0.2146	0.7769
2.5	0.0998	0.4898	0.7837	0.1299	0.2019	0.9157
5	0.1774	1.1369	0.6774	0.2088	1.0068	0.7863
10	0.2429	1.2854	0.7534	0.3452	2.2925	0.6642
15	0.2459	1.4985	0.6932	0.5522	0.2456	0.9445
20	0.3027	2.1699	0.6187	0.6149	0.9012	0.6645
30	0.3894	1.8909	0.7581	0.7478	0.2924	0.9547

first step, adsorbate is adsorb onto the surface of adsorbent through the external surface or prompt adsorption process; in the second step steady adsorption step which shows the controlled intraparticle diffusion, and in the third step, adsorbate transfers from larger pore to micropores consequently decrease in adsorption rate and finally attaining equilibrium step. Another kinetics model including IPDM has also described the mechanism of fluoride adsorption by the adsorbent. The IPDM was proposed by Weber and Morris [49] by Eq. (8):

$$q_t = K_{id}\, t^{1/2} + C \quad (8)$$

Where, K_{id} (mg g^{-1} $min^{-1)}$ is the Intraparticle diffusion rate constant, C (mg g^{-1}) is the thickness of the boundary layer, and the values of K_{id} and C are calculated from the slope and intercept of q_t vs.$t^{1/2}$ plots (Figs. S2 (a) and (b)), respectively. Table 2 shows the obtained value**.** According to IPDM, if the adsorption of a solute is controlled by the intra-particle diffusion process, a plot of q_t versus $t^{1/2}$ passes through the origin. Therefore, it was concluded that intraparticle diffusion are involved in the adsorption of Fluoride onto ACP-250 and ACP-500.

3. 5. Study of Adsorption Thermodynamics

The thermodynamics parameters could be responsible for comprehensive information about the essential energy and structural change after adsorption. The thermodynamics parameters were calculated as Eqs. (9)–(10): the change in Gibbs free energy (ΔG°) (KJ mol^{-1}), where ΔH is the change in enthalpy and ΔS° is the change in entropy.

$$K_c = \frac{q_e}{C_e} \quad (9)$$

$$\Delta G = -RT\, lnK \quad (10)$$

$$ln\, K_c = \frac{\Delta S}{R} - \frac{\Delta H}{RT} \quad (11)$$

where, K_c is the equilibrium constant, q_e is the quantity (mg/g) of fluoride adsorbed on the surface of biosorbent at equilibrium, C_e represents the equilibrium concentration of fluoride in a solution (mg/L), and R denotes the universal gas constant (8.314 J/mol K), while T is the absolute temperature (K) respectively. Fluoride adsorption experiments were completed at different temperatures of (25, 35, 45, and 55) °C, and showed that the removal percentage of fluoride decreased with increased absolute temperature. The changes in enthalpy and entropy were calculated from the plot of ln Kc vs. 1/T, which are shown in Fig. S2 (c) and (d), and Table S2 gives the obtained values. The results show that the adsorption of fluoride depends on temperature. The negative value of ΔG° for ACP-250 represents a non-spontaneous process; however, the value of ΔG° for ACP-500 specifies that the adsorption process favorable at (25 and 35) °C temperature.[50] The process of thermodynamics was exothermic which was confirmed by the negative value of ΔH° and ΔS° means the adsorption decreases with increase in temperature. The opportunity for favorable adsorption can be represented by the negative value of ΔS° for both the bioadsorbents.[51]

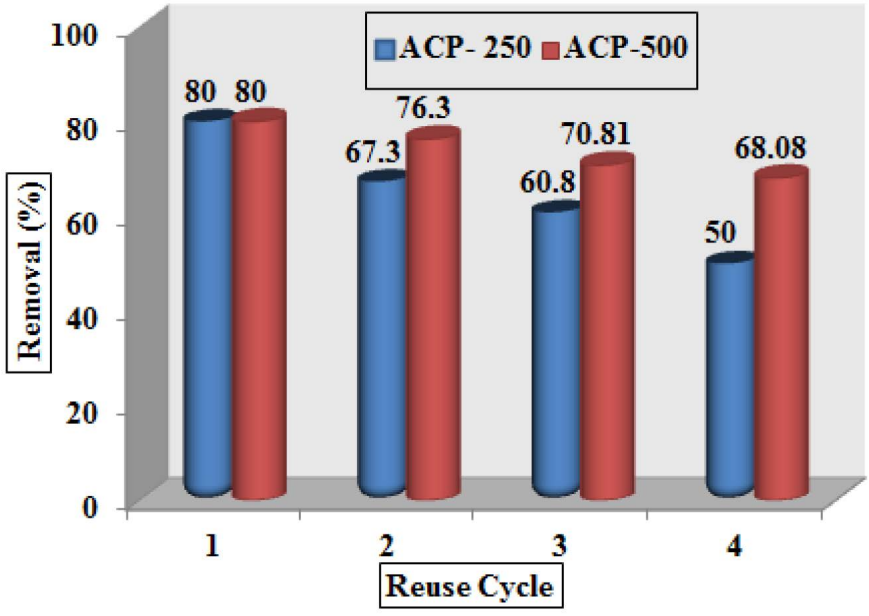

Figure 6. Reusability potential of the synthesized biosorbents (ACP-250 and ACP-500).

4. Regeneration Stability Test

The adsorption and desorption efficiency are the significant characteristics of an adsorbent. The reproducibility of an adsorbent decreases its overall cost, hence increases its value in the continuous batch experiment. The desorption of fluoride from ACP-250 and ACP-500 for the regeneration of active site was performance in 0.1 M sodium hydroxide (NaOH) solution as a desorbing agent for two hours; the adsorbent was then washed with distilled water, until the solution pH became neutral. The regenerated adsorbents (ACP-250 and ACP-500) were tested for fluoride removal from aqueous solution. The regeneration experiment was conducted with a concentration of 5.0 mg L^{-1} of aqueous fluoride solution during the beginning of every cycle. Fig. 6 shows the results of reusability. For the (1^{st} 2^{nd}, 3^{rd}, and 4^{th}) cycle, the removal efficiencies of ACP-500 were (80, 76.3, 70.81, and 68.08)%; however for ACP-250, they were (80, 67.3, 60.8, and 50)%, respectively. The results clearly show that both biosorbents can be reused effectively to remove fluoride ion from water. However, ACP-500 has higher regeneration efficiency, as compared to ACP-250.

6. Comparison of the Fluoride Adsorption Capacity of ACP and other Biomass-Based Absorbents

Comparisons of the maximum fluoride adsorption capacity of ACP-250 and ACP-500 with a wide variety of adsorbent have been reported. Table 3 shows that the Langmuir adsorption capacity of fluoride was (7.58 and 12.63) mg/g) using ACP-250 and ACP-500, respectively, which values are higher than those of activated alumina, wheat straw raw, original tea, *Moringa indica* based activated carbon, activated bagasse carbon, biomass carbon at 300 °C, and biomass carbon at 600 °C based adsorbents. It requires less time (equilibrium-3hrs) to remove almost all amount of fluoride in comparison with some other studies.[52,53] Removal of fluoride was not much affected by pH of the aqueous solution so it can be applied for the removal of fluoride from ground water as well as from wastewater of any pH. For ACP-500 maximum 80.5% removal was observed at pH 4 and at alkaline medium i.e. pH 8, about 56% removal was obtained. While ACP-250 shows good results at pH 4. As shown in the Table 3, it was observed that the adsorbents of present study having higher adsorption capacity than other adsorbent.

Table 3: Comparison of the defluoridation capacities of different biomass based sorbents

Adsorbent	Adsorption capacity (mg/g)	References
Activated alumina	7.6	(Ku and Chiou, 2002)[52]
Wheat straw raw	1.9	(Yadav *et al.,* 2013) [54]
Original tea	3.83	(Caia *et al.,* 2015)[55]
Tea–Fe	10.47	(Caia *et al.,* 2015)[55]
Moringa indica based activated carbon	0.23	(Karthikeyan *et al.,* 2007)[56]
Wheat straw raw	1.93	(Yadav *et al.,* 2013)[54]
Activated bagasse carbon	1.15	(Yadav *et al.,* 2013)[54]
Biomass carbon at 300 °C	0.52	(Sinha *et al.,* 2003)[57]
Biomass carbon at 600 °C	1.54	(Sinha *et al.,* 2003)[57]
Pine wood biochar	7.66	(Mohan *et al.,* 2012)[58]
ACP-250	**7.8247**	**This study**
ACP-500	**13.0039**	**This study**

7. Cost Analysis for Fluoride Removal

The cost of the fluoride treatment by applying biosorbents is dependent on various factors, such as the adsorption efficiency of the adsorbent, reuse capability scale of the application, etc. The present study showed some important efforts of the regeneration and reuse of ACPs in successive cycles, which indicate that ACP-250 and ACP-500 were used to remove fluoride up to four cycles. Table S3 summarizes the cost of some of the material that is used for the removal of fluoride. As the present adsorbent is cost effective and yet it is non-commercial but can be commercialized. *Citrus limetta* pulp alone could not be used directly as an adsorbent for fluoride removal because it leaches in the solution as well as shows negligible adsorption. Hence, modification is done to increase the removal efficiency of the material. Material developed after modification makes adsorbent magnetic and it becomes very easy to separate the adsorbent through magnet and can be recycled many times. The cost of activated carbon prepared from pulp was calculated on the basis of raw material cost and process cost.

8. Conclusion

Low-cost highly efficient magnetic or iron permeated activated carbon (ACP-250 and ACP-500) were synthesized from *Citrus limetta* pulp waste, and applied for the removal of fluoride ions from aqueous solution. FTIR analysis of ACP-250 and ACP-500 confirmed that fluoride-adsorbing groups were present on the surface of biosorbents. EDX results show that carbon was the dominant element in both biosorbents (Carbon content of 58% in ACP-500 and 50.3% in ACP-250. XRD results show that iron was present in the form of oxides and carbide. Slightly acidic pH and 25 °C temperature were favorable for the removal of fluoride from an aqueous solution using magnetically active resource materials. Adsorption of fluoride followed the monolayer Langmuir isotherm model and pseudo-second-order kinetics. This study confirmed that ACP-500 showed higher removal efficiency of fluo-

ride than ACP-250. It was observed that the synthesized bioadsorbent can be used up to four cycles with effective removal of fluoride and the cost analysis proved that the synthesized biogenic iron permeated activated carbon was cost effective. Therefore, waste biomass of *Citrus limetta* could be applied as highly proficient material for the removal of fluoride from the water.

9. Acknowledgment

The authors are grateful to the Science and Engineering Research Board, for providing financial support for this work (Department of Science and Technology (SERB-DST) Sponsored Project No. ECR/2016/001924). Special thanks to the University Sophisticated Instrumentation Center (USIC) BBAU, Lucknow, for their kind support in the characterization of adsorbents. In addition this was partially supported by research grant-2019 of Kwangwoon University, Seoul and Republic of Korea.

10. References

1. M. Amini, K. Mueller, K. C. Abbaspour, T. Rosenberg, M. Afyuni, K. N. Moller, M. Sarr, C. A. Johnson, *Environ. Sci. Technol.* 2008, *42*, 3662–3668. **DOI:**10.1021/es071958y
2. A. L. Srivastav, P. K. Singh, V. Srivastava, Y. C. Sharma, *J. Hazard. Mater.* 2013, *263*, 342–352. **DOI:** 1https://doi.org/10.1016/j.jhazmat.2013.04.017
3. D. Banks, C. Reimann, O. Røyset, H. Skarphagen, O. M. Saether, *Appl. Geochem*. 1995, *10*, 1–16. **DOI:**10.1016/0883-2927(94)00046-9
4. M. Edmunds, P. Smedley, *Elsevier Academic Press Environ. Sci. Technol.* 2005, *34*, 3247–3253.
5. E. J. Reardon, Y. Wang, *Environ. Sci. Technol*. 2000, *34*, 3247–3253. **DOI:** 1https://doi.org/10.1021/es990542k
6. F. Shen, X. Chen, P. Gao, G. Chen, *Chem. Eng. Sci*. 2003, *58*, 987–993. **DOI:**10.1016/S0009-2509(02)00639-5
7. G. Puente, J. J. Pis, J. A. Menéndez, P. J. Grange, *Anal. Appl. Pyrolysis*. 1997, *43*, 125–138. **DOI:**10.1016/S0165-2370(97)00060-0
8. W.H.O. Guidelines for Drinking Water Quality. Geneva. 2004.
9. S. Ayoob, A. K. Gupta, *Environ. Sci. Technol*. 2006, *36*, 433–487. **DOI:**10.1080/10643380600678112
10. B. S. Sharma, J. Agrawal, A. K. Gupta, *Asian J. Environ. Biol.* 2011, *2*, 131–134. **DOI:**10.1021/ie202189
11. M. Mahramanlioglu, I. Kizilcikli, I. O. Bicer, *J. Fluorine Chem.* 2002, *115*, 41–47. **DOI:**10.1016/S0022-1139(02)00003-9
12. P. T. C. Harrison, *J. Fluorine Chem*. 2005, *126*, 1448–1456. **DOI:**10.1016/j.jfluchem.2005.09.009
13. X. Fan, D. J. Parker, M. D. Smith, *Water Res*. 2003, *37*, 4929–4937. **DOI:**10.1016/j.watres.2003.08.014
14. M. G. Sujana, G. Soma, N. Vasumathi, S. Anand, *J. Fluorine Chem.* 2009, *130*, 749–754. **DOI:**10.1016/j.jfluchem.2009.06.005
15. X. Wu, Y. Zhang, X. Dou, M. Yang, *Chemosphere*. 2007, *69*, 1758–1764. **DOI:**10.1016/j.chemosphere.2007.05.075
16. K. Biswas, K. Gupta, A. Goswami, U. C. Ghosh, *Desalination*. 2010, *255*, 44–51. 10.1016/j.desal.2010.01.019. **DOI:**10.1016/j.desal.2010.01.019
17. N. Viswanathan, S. Meenakshi, *Appl. Clay Sci*. 2010, *48*, 607–611. **DOI:**10.1016/j.clay.2010.03.012
18. R. C. Meenakshi, Maheshwari, *J. Hazard. Mater*. 2006, *B137*, 456–463. **DOI:**10.1016/j.jhazmat.2006.02.024
19. J. Wioeniewski, A. Rozanska, *Desalination.* 2007, *212*, 251–260. **DOI:**10.1016/j.desal.2006.11.008
20. S. Deng, H. Liu, W. Zhou, J. Huang, G. Yu, *J. Hazard. Mater*. 2011, *186*, 1360–1366. **DOI:**10.1016/j.jhazmat.2010.12.024
21. A. Bhatnagar, E. Kumar, M. Sillanpaa, *Chem. Eng. J.* 2011, *171*, 811–840. **DOI:**10.1016/j.cej.2011.05.028
22. M. Rafatullah, O. Sulaiman, R. Hashim, A. Ahmad, *J. Hazard. Mater*. 2010, *177(1–3)*, 70–80. **DOI:**10.1016/j.jhazmat.2009.12.047
23. J. R. Koduru, L. P. Lingamdinne, J. Singh, K. H. Choo, *Process Saf. Environ. Prot*. 2016, *103*, 87–96. **DOI:**10.1016/j.psep.2016.06.038
24. Y. Li, N. Li, D. Chen, X. Wang, Z. Xu, D. Dong, 2009, *Water, air, and soil pollut*, *196*(1–4), 41–49. **DOI:**10.1007/s11270-008-9756-2
25. J. Singh, N. S. Mishra, S. Uma Banerjee, Y. C. Sharma, *Bio. Resour.* 2011, *6(3)*, 2732–2743.
26. H. Paudyala, B. Pangenia, K. Inouea, H. Kawakitaa, K. Ohtoa, H. Haradaa, S. Alam, *J. Hazard. Mater.* 2011, *192*, 676–682. **DOI:**10.1016/j.jhazmat.2011.06.068
27. H. Li, Z. Li, T. Liu, X. Xiao, Z. Peng, L. Deng, *Bioresour. Technol.* 2008, *99*, 6271–6279. **DOI:**10.1016/j.biortech.2007.12.002
28. S. Srivastavaa, S. B. Agrawala, M. K. Mondalb, *Ecol. Eng.* 2015, *85*, 56–66. **DOI:**10.1016/j.ecoleng.2015.10.011
29. Lambert, J. B (1987). Macmillan, New York
30. L. H. V. Jimenez, R. H. Hurt, J. Matos, J. R. R. Mendez, *Environ. Sci. Technol*. 2014, *48*, 1166–1174. **DOI:**10.1021/es403929b
31. L. Batistella, L. D. Venquiaruto, M. D. Luccio, J. V. Oliveira, S. B. C. Pergher, M. A. Mazutti, D. de Oliveira, A. J Mossi, H. Treichel, R. Dallago, *Ind. Eng. Chem. Res.* 2011, *50*, 6871–6876. **DOI:**10.1021/ie101020r
32. J. Sun, S. Zhou, P. Hou, Y. Yang, J. Weng, X. Li, M. Li, *J. Biomed. Mater. Res*. 2006, *80A*, 333–341. **DOI:**10.1002/jbm.a.30909
33. S. Shukla, V. Arora, A. Jadaun, J. Kumar, N. Singh, V. K. Jain, *Int J. Nanomedicine. J.* 2015, *10*, 4901–17. **DOI:**10.2147/IJN.S77675
34. C. Gai, F. Zhang, Q. Lang, T. Liu, N. Peng, Z. Liu, *Appl. Catal. B: Environ*. 2017, *204*, 566–576. **DOI:**10.1016/j.apcatb.2016.12.005
35. S. Dwivedi, P. Mondal, C. Balomajumder, *Res. J. Chem. Sci.* 2014, *4(1)*, 50–58.
36. T. P. Singh, C. B. Majumder, *Int. J. Pharm. Pharm. Sci.* 2016, *8*, 8–7. **DOI:**10.22159/ijpps.2016v8i10.12253
37. S. Karthikeyan, R. Balasubramanian, C. S. P. Iyer, *Bioresour. Technol*. 2007, *98*, 452–455.

DOI:10.1016/j.biortech.2006.01.010
38. M. D. Meitei, M. N. V. Prasad, *Ecol. Eng.* 2014, *71*, 308–317. **DOI:**10.1016/j.ecoleng.2014.07.036
39. D. Tang, G. Zhang, *Chem. Eng. J.* 2016, *283*, 721–729. **DOI:**10.1016/j.cej.2015.08.019
40. D. P. Das, J. Das, K. Parida, *J. Colloid Interface Sci*. 2003, *261*, 213–220. **DOI:**10.1016/S0021-9797(03)00082-1
41. I. J. Langmuir, *Am. Chem. Soc.* 1916, *38*, 2221–2295. **DOI:**10.1021/ja02268a002
42. H. Freundlich, 1906, *57*, 385–470. **DOI:**10.4236/ojn.2015.56057
43. S. Kundu, A. K. Gupta, *Chem. Eng. J*. 2006, *122(1–2)*, 93–106. **DOI:**10.1016/j.cej.2006.06.002
44. E. Bulut, M. Ozacar, I. A. Sengil, *J. Hazard. Mater*. 2008, *154*, 613–622. **DOI:**10.1016/j.jhazmat.2007.10.071
45. E. Demirbas, M. Kobya, A. E. S. Konukman, *J. Hazard. Mater*. 2008, *154*, 787–794. **DOI:**10.1016/j.jhazmat.2007.10.094
46. Y. S. Ho, G. Mckay, *Process Saf. Environ. Prot*. 1998, *76*, 332–340. **DOI:**10.1205/095758298529696
47. Y. S. Ho, D. A. J. Wase, C. F. Forster, *Water Res.* 1995, *29*, 1327–1332. **DOI:**10.1016/0043-1354(94)00236-Z
48. F. C. Wu, R. L. Tseng, R. S. Juang, *Chem. Eng. J.* 2009, *153*, 1–8. **DOI:**10.1016/j.cej.2009.04.042
49. J. W. J. Weber, J. C. Morris, *J. Sanit. Eng. Div. ASCE.* 1963; *89(SA2)*, 31–59.
50. J. Singh, K. J. Reddy, Y. Y. Chang, S. H. Kang, J. K. Yang, *Process Saf. Environ. Prot.* 2016, *99*, 88–97. **DOI:**10.1016/j.psep.2015.10.011
51. M. E. Mahmoud, G. M. Nabil, N. M. El-Mallah, H. I. Bassiouny, S. Kumar, T. M. Abdel-Fattah, *J. Ind. Eng. Chem.* 2016, *37*, 156–167. **DOI:**10.1016/j.jiec.2016.03.020
52. Y. Ku, H. Chiou, *Water Air Soil Pollut.* 2002, *133*, 349–361. **DOI:**10.1023/A:1012929900113
53. H. Huang, J. Liu, P. Zhang, D. Zhang, F. Gao, *Chem. Eng. J.* 2017, *307,* 696–706. **DOI:**10.1016/j.cej.2016.08.134
54. A. K. Yadav, R. Abbassi, A. Gupta, M. Dadashzadeh, *Ecol. Eng*. 2013, *52*, 211–218. **DOI:**10.1016/j.ecoleng.2012.12.069
55. H. M Caia, G. J. Chena, C. Y. Penga, Z. Z. Zhanga, Y. Y. Donga, G. Z. Shanga, X. H. Zhua, H. J. Gaob, X. C. Wana, *Appl. Surf. Sci*. 2015, *328*, 34–44. **DOI:**134-44. 10.1016/j.apsusc.2014.11.164
56. G. Karthikeyan, S. S. Llango, *Iran. J. Environ. Healt. Sci. Eng.* 2007, *4*, 21–28.
57. S. Sinha, K. P. Pandey, D. Mohan, K. P. Singh, *Ind. Eng. Chem. Res*. 2003, *42*, 6911–6918. **DOI:**10.1021/ie030544k
58. D. Mohan, R. Sharma, V. K. Singh, P. Steele, C. U. Pittman, *Ind. Eng. Chem. Res.* 2012, *51*, 900–914. **DOI:**10.1021/ie202189v

Povzetek

Tekom študije smo uspešno sintetizirali biogeni aktivni ogljik iz ostankov pulpe limete (*Citrus limetta*) in ga uporabili za odstranjevanje fluoridnih ionov iz vodne raztopine. Za sintezo aktivnega oglja smo surovino segreli v pečici pri dveh različnih temperaturah (250 °C in 500 °C) in vzorca označili kot ACP-250 in ACP-500. Pripravljen biosorbent smo karakterizirali z vrstično elektronsko mikroskopijo (SEM), infrardečo spektroskopijo s Fourierjevo transformacijo (FTIR) in rentgensko difrakcijo (XRD). Šaržne študije adsorpcije smo izvedli pri različnih temperaturah, količini, pH vrednostih in začetnih pogojih. Za razumevanje adsorpcijskega mehanizma smo določili adsorpcijske izoterme in reakcijsko kinetiko. Rezultati študije so pokazali, da je bila maksimalna odstranjena količina ionov znašala za ACP-500 86 % in za ACP-250 82 %. Izoterme najbolje opišemo z Langmuirjevo izotermo, z enoslojno adsorpcijsko kapaciteto fluoridnih ionov 12.6 mg/g. Vendar pa kinetiko vezave dobro opišemo kot reakcijo psevdo-drugega reda. Sintetizirani material je bil učinkovit za odstranjevanje fluoridinih ionov iz vode pri različnih temperaturah in bil uporaben tri do štirikrat.